

# Direct Synthesis of Hydrogen Peroxide from H<sub>2</sub> and O<sub>2</sub> Using Al<sub>2</sub>O<sub>3</sub> Supported Au–Pd Catalysts

Benjamin E. Solsona,<sup>†</sup> Jennifer K. Edwards,<sup>†</sup> Philip Landon,<sup>†</sup> Albert F. Carley,<sup>†</sup>  
Andrew Herzing,<sup>‡</sup> Christopher J. Kiely,<sup>‡</sup> and Graham J. Hutchings<sup>\*,†</sup>

School of Chemistry, Cardiff University, Main Building, Park Place, Cardiff, United Kingdom CF10 3AT,  
and Center for Advanced Materials and Nanotechnology, Lehigh University, 5 East Packer Avenue,  
Bethlehem, Pennsylvania 18015-3195

Received November 29, 2005. Revised Manuscript Received February 13, 2006

The direct synthesis of hydrogen peroxide from H<sub>2</sub> and O<sub>2</sub> using a range of alumina supported Au, Pd, and Au–Pd metal catalysts is described and discussed in detail for both fresh catalysts and materials that have been aged in storage. The conditions previously identified as being optimal for hydrogen peroxide synthesis (i.e., low temperatures (2 °C) and short reaction residence times) are employed, and the effect of catalyst composition and preparation was investigated in detail for the fresh catalysts. The addition of Pd to the Au catalyst increases the rate of hydrogen peroxide synthesis as well as the concentration of hydrogen peroxide formed. Interestingly, the addition of relatively small amounts of Pd to the Au/Al<sub>2</sub>O<sub>3</sub> catalyst, replacing up to 20% of the Au, significantly increases the formation of hydrogen peroxide. The microstructure of the catalysts was studied using transmission electron microscopy and X-ray photoelectron spectroscopy for both the fresh and the aged catalyst, and the supported bimetallic particles were found to be of core–shell morphology with a Pd-rich surface. Hence, relatively little Pd is needed to induce the enhanced catalytic formation of hydrogen peroxide. Calcination at 400 °C leads to the formation of stable reusable catalysts, whereas lower temperature pretreatments generate unstable catalysts that leach both Au and Pd into solution. Catalysts that have been aged in storage give an increase in activity for hydrogen peroxide synthesis by a factor of ca 3, and the relationship between the catalyst structure and this activity is discussed. The catalysts were also investigated for CO oxidation at 25 °C, and all were found to be inactive or almost inactive; similarly, catalysts that are very effective for low-temperature CO oxidation were found to be totally inactive for H<sub>2</sub> oxidation to H<sub>2</sub>O<sub>2</sub>. This suggests an inverse correlation between catalysts that are active for either CO or H<sub>2</sub> activation, and this is commented on with respect to the mechanism.

## Introduction

The direct synthesis of hydrogen peroxide from the oxidation of molecular hydrogen by molecular oxygen is considered to be of immense current interest. Hydrogen peroxide is a noted green oxidant that is useful in many large scale processes such as bleaching and as a disinfectant. Its use in the fine chemical industry accounts for a much lower consumption, but since it is viewed as a green oxidant with water being the only byproduct, it is recognized to have significant potential in chemical synthesis, particularly in the production of propene oxide using the microporous redox catalyst titanium silicalite TS-1.<sup>1,2</sup> In addition, it is probable that hydrogen peroxide can replace stoichiometric (i.e., noncatalytic) oxygen donors in a number of processes. At present, hydrogen peroxide is produced by the sequential hydrogenation and oxidation of an alkyl anthraquinone,<sup>3</sup> a

process that is only economic at a large scale. In contrast, most uses of hydrogen peroxide require relatively small amounts. Hence, there is a significant mismatch between the current scales of production and usage. The direct small scale production of hydrogen peroxide at the site where it is used would offer many advantages, least of all that this will negate the need to transport concentrated solutions of hydrogen peroxide. At present, no commercial process exists for the direct formation of H<sub>2</sub>O<sub>2</sub>, but there has been significant interest in this reaction in industrial laboratories for over 90 years.<sup>4</sup> Until very recently, the catalysts used in these investigations have been based on Pd, and since many researchers have concluded that it is important to try to achieve the highest rate of product formation, most of these earlier studies used H<sub>2</sub>/O<sub>2</sub> mixtures in the explosive region; solutions of over 35 wt % hydrogen peroxide have been made by reacting H<sub>2</sub>/O<sub>2</sub> over Pd catalysts at elevated pressures.<sup>5</sup> However, operating in the explosive region with H<sub>2</sub>/O<sub>2</sub> mixtures can be considered extremely dangerous, and more recently, studies have concentrated on carrying out the

\* Corresponding author. Tel.: +44 (0)2920874805. Fax: +44 (0)2920874075.  
E-mail: hutch@cardiff.ac.uk.

<sup>†</sup> Cardiff University.

<sup>‡</sup> Lehigh University.

(1) Chen, L. Y.; Chauh, G. K.; Jaenicke, J. *J. Mol. Catal. A* **1999**, *132*, 281.

(2) Lin, W.; Frei, H. *J. Am. Chem. Soc.* **2002**, *124*, 9292.

(3) Hess, H. T. *Kirk-Othmer Encyclopaedia of Chemical Engineering*; John Wiley & Sons: New York, 1995.

(4) Henkel, H.; Weber, W. Manufacture of hydrogen peroxide. U.S. Patent 1,108,752, 1914.

(5) Gosser, L. W.; Schwartz, J.-A. T. Catalytic process for making hydrogen peroxide from hydrogen and oxygen employing a bromide promoter. U.S. Patent 4,772,458, 1988.

reaction with dilute  $\text{H}_2/\text{O}_2$  mixtures well away from the explosive region.<sup>6,7</sup>

In our preceding papers concerning the direct synthesis of  $\text{H}_2\text{O}_2$ , we have shown that catalysts based on Au–Pd alloys supported on alumina can give rather significant improvements in the rate of hydrogen peroxide formation when compared with the Pd-only catalyst.<sup>8,9</sup> Recently, we have shown that  $\text{TiO}_2$  and  $\text{Fe}_2\text{O}_3$  can also be used as supports, and with these catalysts, the optimum formulation for hydrogen peroxide synthesis is 2.5 wt % Au and 2.5 wt % Pd coimpregnated onto the support.<sup>10,11</sup> In this paper, we extend our initial studies using the alumina supported catalysts and show that only a relatively small amount of palladium is required to achieve a significant enhancement in the rate of hydrogen peroxide synthesis with this support. Furthermore, we demonstrate that aging of the  $\text{AuPd}/\text{Al}_2\text{O}_3$  material increases the catalyst activity significantly, and we show the structural features of the catalysts responsible for this effect.

## Experimental Procedures

**Catalyst Preparation.** 5 wt %  $\text{Pd}/\text{Al}_2\text{O}_3$ , 5 wt %  $\text{Au}/\text{Al}_2\text{O}_3$ , and a range of Au–Pd/ $\text{Al}_2\text{O}_3$  catalysts were prepared by impregnation of  $\gamma\text{-Al}_2\text{O}_3$  (Condea SCF-140) via an incipient wetness method using aqueous solutions of  $\text{PdCl}_2$  (Johnson Matthey) and/or  $\text{HAuCl}_4 \cdot 3\text{H}_2\text{O}$  (Johnson Matthey). For the 2.5 wt % Au–2.5 wt %  $\text{Pd}/\text{Al}_2\text{O}_3$  catalyst, the detailed procedure was as follows: an aqueous solution (10 mL) of  $\text{HAuCl}_4 \cdot 3\text{H}_2\text{O}$  (5 g in 250 mL of water) and an aqueous  $\text{PdCl}_2$  solution (4.15 mL of a solution of 1 g in 25 mL of water) were simultaneously added to  $\gamma$ -alumina (3.8 g). The paste formed was ground and dried at 120 °C for 16 h and finally calcined in static air at 400 °C for 3 h. Other Au–Pd ratios were prepared by varying the amounts of reagents accordingly. The catalysts were pretreated using a range of conditions: drying at 80 °C in air for 3 h, calcination in static air at 400 °C for 3 h, and reduction in flowing  $\text{H}_2$  (5 wt %  $\text{H}_2$  in Ar) at 500 °C. Catalysts were used fresh (i.e., within a few hours of synthesis). A sample of the 2.5 wt % Au–2.5 wt %  $\text{Pd}/\text{Al}_2\text{O}_3$  catalyst was stored in a sealed container for 12 months prior to retesting.

**Catalyst Testing.** Hydrogen peroxide synthesis was performed using a Parr Instruments stainless steel autoclave with a nominal volume of 50 mL and a maximum working pressure of 14 MPa. The autoclave was equipped with an overhead stirrer (0–2000 rpm) and provision for measurement of temperature and pressure. Typically, the autoclave was charged with catalyst (0.05 g unless otherwise stated) and solvent (5.6 g of MeOH and 2.9 g of  $\text{H}_2\text{O}$ ), purged 3 times with  $\text{CO}_2$  (3 MPa), and then filled with 5%  $\text{H}_2/\text{CO}_2$  and 25%  $\text{O}_2/\text{CO}_2$  to give a hydrogen-to-oxygen ratio of 1:2,

at a total pressure of 3.7 MPa at 2 °C. Stirring (1200 rpm unless otherwise stated) began when the desired temperature was reached, and experiments were run for 30 min unless otherwise stated.  $\text{H}_2\text{O}_2$  yield was determined by titration of aliquots of the final filtered solution with acidified  $\text{Ce}(\text{SO}_4)_2$  ( $7 \times 10^{-3}$  mol/L).  $\text{Ce}(\text{SO}_4)_2$  solutions were standardized against  $(\text{NH}_4)_2\text{Fe}(\text{SO}_4)_2 \cdot 6\text{H}_2\text{O}$  using ferroin as indicator. The rate of hydrogen peroxide formation was determined for all catalysts at 30 min and is expressed as mol of  $\text{H}_2\text{O}_2$  produced per unit mass of catalyst per unit time, and this is used to compare catalyst effectiveness.

The catalytic activity for CO oxidation was determined in a fixed bed quartz microreactor, operated at atmospheric pressure. The feed consisted of  $\text{CO}/\text{O}_2/\text{N}_2$  with a molar ratio of 0.5/19.9/79.6. The combined flow rate was maintained at 22.5 mL  $\text{min}^{-1}$ , and a constant catalyst loading of 50 mg was employed. The catalyst temperature was maintained at 25 °C by immersing the quartz bed in a thermostatically controlled water bath. Catalysts were tested for a minimum of 500 min, and analysis of the reaction product was carried out on-line using gas chromatography. Conversion was calculated on the basis of  $\text{CO}_2$  concentration in the effluent, and carbon balances were  $100 \pm 2\%$ .

**Catalyst Characterization.** Au and Pd concentrations were determined using atomic absorption spectroscopy (AAS). AAS was performed with a Perkin-Elmer 2100 atomic absorption spectrometer using an air–acetylene flame. Gold/palladium samples were run at wavelengths of 242.8 nm (Au) and 247.6 nm (Pd). Samples for analysis were prepared by dissolving 0.1 g of the dried catalyst in an aqua regia solution followed by the addition of 250 mL of deionized water to dilute the sample. AAS was used to determine the weight % of the metal incorporated into the support after impregnation and also the concentration (ppm) of Au or Pd that had leached out into solution during reaction by determining the Au and Pd content of the used catalyst and comparing it to the fresh catalyst.

Samples for scanning transmission electron microscopy (STEM) examination were prepared by dispersing the catalyst powder in high-purity ethanol, then allowing a drop of the suspension to evaporate on a holey carbon film supported by a 300 mesh copper TEM grid. Samples were subjected to chemical microanalysis and annular dark-field STEM imaging in a VG systems HB603 STEM operating at 300 kV fitted with an Oxford Instruments INCA TEM 300 system for energy-dispersive X-ray (EDS) analysis. The effective electron probe size and dwell time used in STEM-XEDS mapping experiments was 1.5 nm and 200 ms per pixel, respectively.

X-ray photoelectron spectra were recorded on a VG EscaLab 220i spectrometer, using a standard Al  $\text{K}\alpha$  X-ray source (300 W) and an analyzer pass energy of 20 eV. Samples were mounted using double-sided adhesive tape, and binding energies are referenced to the C(1s) binding energy of adventitious carbon contamination taken to be 284.7 eV.

## Results and Discussion

**Effect of Au–Pd Ratio on Hydrogen Peroxide Synthesis Using Fresh Catalysts.** Au, Pd, and Au–Pd catalysts supported on  $\gamma\text{-Al}_2\text{O}_3$  were prepared using impregnation methods, and these were evaluated, after the catalysts had been calcined at 400 °C, for the synthesis of  $\text{H}_2\text{O}_2$  and the oxidation of CO. The results shown in Table 1, for fresh catalysts, demonstrate that the catalysts are active for  $\text{H}_2\text{O}_2$  synthesis but are totally inactive for CO oxidation. This is a general observation for all supported Au catalysts that we have studied to date. As noted in our earlier studies,<sup>8,9</sup> the pure Au catalysts generate  $\text{H}_2\text{O}_2$  but at low rates. The

- (6) van Weynbergh, J.; Schoebrechts, J.-P.; Colery, J.-C. Direct synthesis of hydrogen peroxide by heterogeneous catalysis, catalyst for the said synthesis and method of preparation of the said catalyst. U.S. Patent 5,447,706, 1995.
- (7) Zhou, B.; Lee, L.-K. Catalyst and process for direct catalytic production of hydrogen peroxide ( $\text{H}_2\text{O}_2$ ). U.S. Patent 6,168,775, 2001.
- (8) Landon, P.; Collier, P. J.; Papworth, A. J.; Kiely, C. J.; Hutchings, G. J. *Chem. Commun.* **2002**, 2058.
- (9) Landon, P.; Collier, P. J.; Chadwick, D.; Papworth, A. J.; Burrows, A.; Kiely, C. J.; Hutchings, G. J. *Phys. Chem. Chem. Phys.* **2003**, *5*, 1917.
- (10) Edwards, J. K.; Solsona, B.; Landon, P.; Carley, A. F.; Herzing, A.; Kiely, C. J.; Hutchings, G. J. *J. Catal.* **2005**, *236*, 69.
- (11) Edwards, J. K.; Solsona, B.; Landon, P.; Carley, A. F.; Herzing, A.; Watanabe, M.; Kiely, C. J.; Hutchings, G. J. *J. Mater. Chem.* **2005**, *15*, 4595.

**Table 1. Hydrogen Peroxide Synthesis Using Catalysts Prepared by Impregnation<sup>a</sup>**

catalyst	calcination treatment	productivity (mol of $H_2O_2$ /h/kg <sub>cat</sub> )	$H_2O_2$ (wt %)	$CO$ conversion (%)
5% Au/ $Al_2O_3$	air 400 °C	2.6	0.0026	<1
4.2% Au0.8% Pd/ $Al_2O_3$	air 400 °C	17	0.017	<1
2.5% Au2.5% Pd/ $Al_2O_3$	air 400 °C	15	0.015	<1
5% Pd/ $Al_2O_3$	air 400 °C	9	0.009	<1
5% Au/ $Al_2O_3$	air 400 °C + $H_2$ 500 °C	1	0.001	<1
4.2% Au0.8% Pd/ $Al_2O_3$	air 400 °C + $H_2$ 500 °C	21	0.021	<1
2.5% Au2.5% Pd/ $Al_2O_3$	air 400 °C + $H_2$ 500 °C	9.3	0.093	<1
5% Pd/ $Al_2O_3$	air 400 °C + $H_2$ 500 °C	6	0.006	<1

<sup>a</sup> 50 mg of catalyst was used in all experiments.

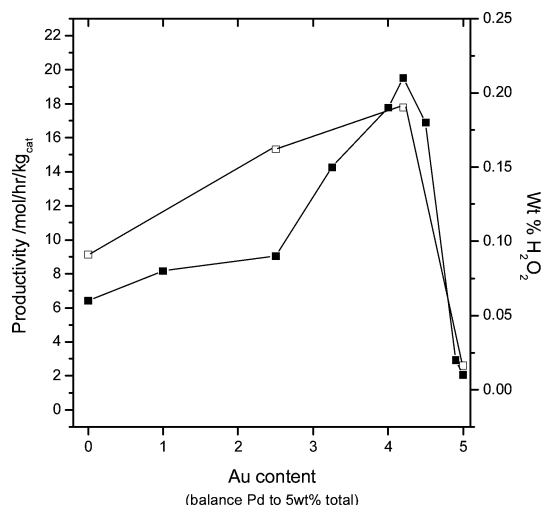


**Figure 1.** Effect of addition of Au to supported Pd/ $Al_2O_3$  catalysts for the synthesis of hydrogen peroxide. Catalysts calcined at 400 °C in air (□) or calcined in air at 400 °C and reduced at 500 °C with hydrogen (■). Mass of catalyst = 50 mg.

addition of Pd to Au significantly enhances the catalytic performance for the synthesis of  $H_2O_2$ , and moreover, it is interesting to note that there is an optimum Pd–Au composition (Pd/Au ~ 1:5) where the rate of  $H_2O_2$  production is much higher than for the pure Pd catalyst, which in itself is significantly more active than pure gold. It is apparent that the addition of Pd to Au also enhances the selectivity to  $H_2O_2$ , and the enhanced rate of  $H_2O_2$  synthesis is achieved at lower  $H_2$  conversion.

A series of Au–Pd/ $Al_2O_3$  catalysts was prepared using the impregnation method, calcined at 400 °C, and then reduced in  $H_2$  at 500 °C. This is similar to the method of catalyst preparation that was used in our initial studies with Au–Pd/ $Al_2O_3$  catalysts.<sup>8,9</sup> The results (Figure 1) show that reduction following calcination increases the rate of  $H_2O_2$  synthesis for the optimum Au–Pd composition but decreases the rate for all other compositions. A large number of formulations were investigated, and the results confirm that a composition of 4.2 wt % Au–0.8 wt % Pd gives the highest catalytic performance.

We have also investigated the effect of treating the catalysts at lower temperatures prior to use, and this can lead to improved catalytic performance. However, a key consideration for heterogeneous catalysts operating in three phase systems is whether active components leach into the reaction mixture; this may lead to catalyst deactivation or, in the most extreme case, may lead to the formation of an active homogeneous catalyst.<sup>12</sup> To demonstrate that the supported gold/palladium catalysts functioned as wholly heterogeneous

**Table 2. Influence of the Calcination Temperature on Leaching of Gold and Palladium in 2.5% Au2.5% Pd/ $Al_2O_3$  Catalysts after Reaction**

pretreatment	run	loss of Au (%) <sup>a</sup>	loss of Pd (%) <sup>a</sup>	productivity (mol/kg/h)
air, 25 °C,	1	75	79	65
	2	80	85	41
air, 400 °C, 3 h	1	0	0	22
	2	0	0	22

<sup>a</sup> (Gold or palladium present in the fresh catalyst – gold or palladium after runs 1 or 2)/(gold or palladium present in the fresh catalyst) × 100.

catalysts, an experiment was carried out using a 2.5 wt % Au–2.5 wt % Pd/ $Al_2O_3$  catalyst (calcined at 400 °C), and the yield of  $H_2O_2$  was determined. Following this reaction, the catalyst was removed by careful filtration, and the solution was used for a second experiment using  $O_2/H_2$ . No further  $H_2O_2$  was generated, and this indicates that the formation of hydrogen peroxide involves gold acting as a wholly heterogeneous catalyst. Indeed, the catalysts that had been calcined at 400 °C could be reused without loss of performance (Table 2), and AAS analyses confirmed that there was no loss of Au or Pd from the sample during use. In contrast, the uncalcined Au–Pd/ $Al_2O_3$  catalysts were particularly unstable and could not be reused effectively (Table 2). AAS analysis showed that for the uncalcined catalyst, almost all the Au and Pd was lost during the initial usage, giving rise to a decrease in activity during a second use. It should be noted that proportionately, the loss of metals by leaching is much larger than the decrease in productivity for hydrogen peroxide formation. This suggests that more effective catalysts may be produced for this reaction by careful control of the catalyst preparation methodology. At present, effective catalysts have been prepared using co-impregnation of the metal salts directly onto the support. Interestingly, as yet we have not been able to produce effective catalysts using coprecipitation or deposition precipitation, and this preparative aspect is clearly an area for further investigation.

**Catalyst Characterization of Fresh Catalysts.** To determine the nature of the alumina supported Au/Pd catalysts, a detailed investigation of freshly prepared catalysts was carried out using electron microscopy and X-ray photoelectron spectroscopy. In our previous study, we initially explored the microstructure of the calcined and reduced samples and demonstrated that the addition of Pd to Au produces Au–Pd alloys over the whole range of particle sizes observed.<sup>8,9</sup>

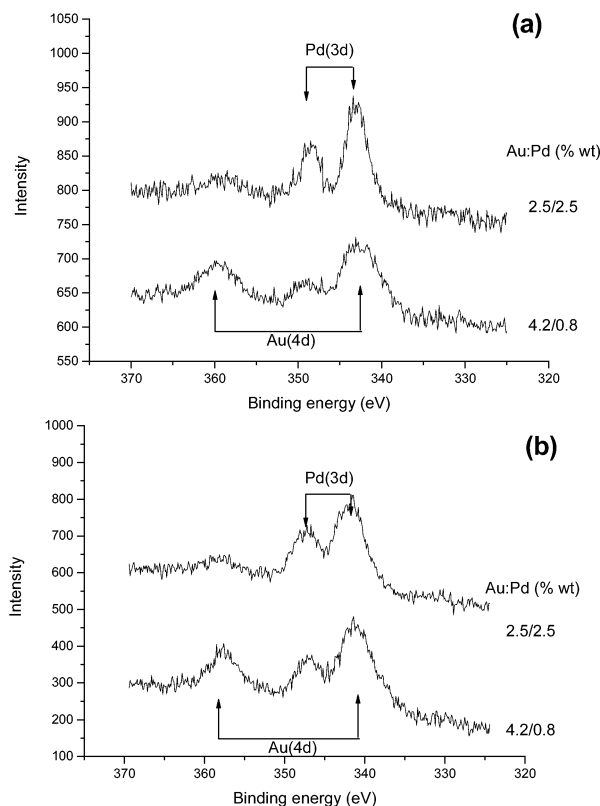


**Figure 2.** Au(4d) and Pd(3d) spectra for two Au–Pd/Al<sub>2</sub>O<sub>3</sub> catalysts (compositions as shown) (a) dried at 120 °C and (b) calcined at 400 °C.

**Table 3.** Comparison of Measured (XPS) and Expected Pd/Au Ratios for Two Au–Pd/Al<sub>2</sub>O<sub>3</sub> Catalysts

composition	heat treatment	Pd/Au molar ratio	
		measured	theoretically expected (for random solid solution)
4.2% Au–0.8% Pd	dried 120 °C	0.23	0.35
	calcined 400 °C	0.50	0.35
2.5% Au–2.5% Pd	dried 120 °C	1.65	1.86
	calcined 400 °C	3.06	1.86

We now investigate the nature of the structure of these active catalysts further.

The Au(4d)–Pd(3d) XPS spectra for the two most active Au–Pd/Al<sub>2</sub>O<sub>3</sub> catalysts (with compositions of 4.2 wt % Au–0.8 wt % Pd and 2.5 wt % Au–2.5 wt % Pd) are shown in Figure 2 for the uncalcined and calcined (400 °C) samples. Because of the overlap between the Au(4d<sub>5/2</sub>) and the Pd(3d) signals, to estimate the Au/Pd molar ratios, we must first calculate the intensity of the former using the Au(4d<sub>3/2</sub>) peak intensity and the known intensity ratio of the spin–orbit components. This is then subtracted from the measured Pd(3d) peak intensity and the Pd(3d)/Au(4d<sub>5/2</sub>) ratio corrected using the sensitivity factors of Wagner<sup>13</sup> to obtain the surface Pd/Au molar ratio. For both samples, the uncalcined catalysts exhibit a Pd/Au ratio lower than that expected from the known composition (assuming a random solid solution), but calcination in air at 400 °C apparently leads to a surface enrichment in Pd (Table 3).

STEM and XEDS results for the fresh calcined 2.5 wt % Au–2.5 wt % Pd/Al<sub>2</sub>O<sub>3</sub> catalyst reported previously<sup>9</sup> showed that this sample is comprised of well-dispersed fcc metal particles with a size range of between 2 and 10 nm with the

majority being at the lower end of the size range. Detailed STEM and EDS analysis showed that the particles all were comprised of both Au and Pd and that the ratio of Au/Pd was ca. 1:1 with a slight enrichment of Pd in the larger particles. Very few particles over 10 nm in diameter were observed in the fresh catalyst

**Catalyst Characterization of Aged Catalysts.** We decided to study the effect of storage on catalyst activity as, typically, catalyst performance declines with storage for many catalysts. We stored a sample of the most active 2.5 wt % Au–2.5 wt % Pd/Al<sub>2</sub>O<sub>3</sub> catalyst, which had been previously calcined at 400 °C, in a sealed container in the dark for 12 months at ambient conditions. Reevaluation of the catalytic performance of this catalyst showed that under the standard reaction conditions, the activity of the sample had increased from 15 mol of H<sub>2</sub>O<sub>2</sub>/h/kg<sub>cat</sub> (Table 1) to 52 mol of H<sub>2</sub>O<sub>2</sub>/h/kg<sub>cat</sub>, representing a dramatic increase in productivity, and this is similar to the activity we have previously observed with TiO<sub>2</sub> supported catalysts.<sup>10</sup> It has been reported elsewhere that the impregnation process does not produce a very strong bond between metal particle and oxide support.<sup>14</sup> If the atomic mobilities of the gold and palladium were sufficient, then the atoms would be able to agglomerate and grow over time, producing ever larger Au–Pd particles. To investigate this, we reexamined the stored catalyst using annular dark field (ADF) STEM imaging. It was found (Figure 3a) that the sample now exhibited a bimodal size distribution. The smallest particles once again fell into the 3–10 nm size range (mean diameter = 3.6 nm), but also present were some considerably larger particles that ranged in size from 35 to 50 nm (mean diameter = 38 nm). The time lapse between these two studies may suggest that a time-dependent growth process is occurring. STEM-XEDS analyses of this Au–Pd catalyst were also performed, and typical chemical maps shown in Figure 3b,c show the existence of a Au–Pd alloy as well as occasional very small Pd-only particles. It was found that nearly all of the particles tended to be Au–Pd alloys and that the composition of the particles was size-dependent. In general, the smaller the particle, the more Pd-rich and Au-deficient the particle becomes. No pure gold particles were detected.

Closer inspection of one of the larger alloy particles (Figure 4a) suggests that a slight discrepancy exists between the spatial extent of the Pd L<sub>α</sub> and the Au M<sub>2</sub> signals (Figure 4b,c) (i.e., the Pd X-ray signal seems to originate from a larger area than the gold signal). This is most clearly observed in the digitally colored RGB image (Figure 4d), which shows a predominance of the Pd (blue) signal at the perimeter of the particle. These data imply that there is a tendency for Pd surface segregation to occur in the calcined alloy particles, as was also indicated by the XPS data for the fresh sample and has also been found for Au–Pd bimetallic catalysts supported on TiO<sub>2</sub><sup>10</sup> and Fe<sub>2</sub>O<sub>3</sub>.<sup>11</sup> The formation of such Au–Pd core–shell structures has been reported previously for ligand-stabilized bimetallic Au–Pd

(13) Wagner, C. D.; Davis, L. E.; Zeller, M. V.; Taylor, J. A.; Raymond, R. M.; Gale, L. H. *Surf. Interface Anal.* **1981**, 3, 211.

(14) Poole, C. P., Jr.; Owens, F. J. *Introduction to Nanotechnology*; John Wiley & Sons: New York, 2003.

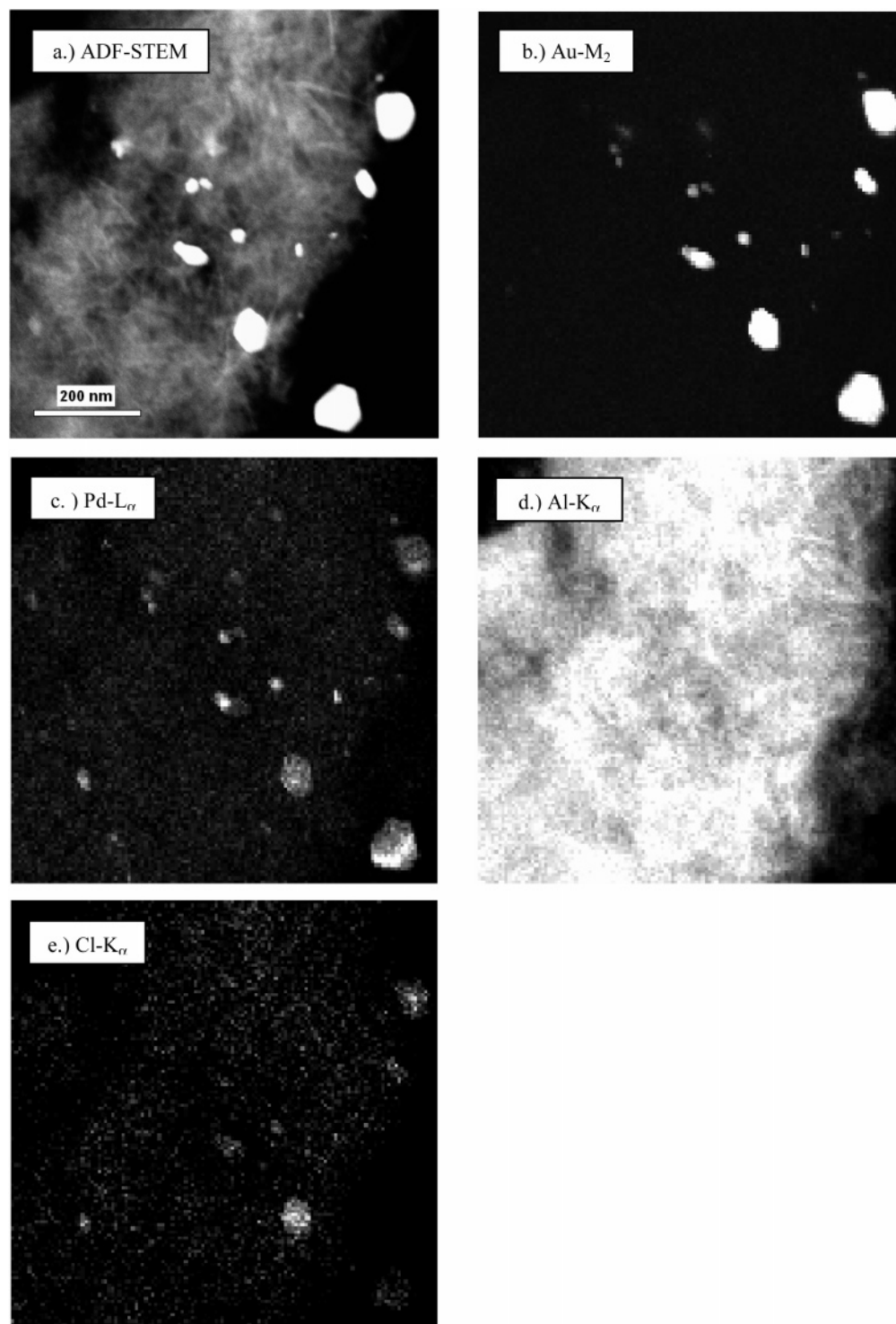


**Figure 3.** Montage of STEM data from the calcined 2.5 wt % Au–2.5 wt % Pd/Al<sub>2</sub>O<sub>3</sub> sample. (a) ADF image and corresponding XEDS maps using (b) Au M<sub>2</sub>, (c) Pd L<sub>α</sub>, (d) Al K<sub>α</sub>, and (e) Cl K<sub>α</sub> signals.

colloids,<sup>15</sup> and in the preparation of bimetallic nanoparticles by the sonochemical reduction of solutions containing gold and palladium ions.<sup>16</sup> These core–shell particles exhibited superior catalytic activity as compared with Au–Pd alloy particles, which had the same overall Au/Pd atom ratio.<sup>16</sup> Detailed <sup>197</sup>Au Mössbauer studies confirmed the presence of a pure Au core, and there was also evidence for a thin alloy region at the interface between the Au core and the Pd

shell.<sup>16,17</sup> Hence, we now consider that our observations are consistent with these previous studies and that the stable Au–Pd/Al<sub>2</sub>O<sub>3</sub> catalysts prepared by calcination at 400 °C are comprised of Au–Pd alloys in which the surface of the nanoparticles is Pd-rich. In this way, it appears that Au electronically promotes Pd for the direct oxidation reaction, and this leads to the enhanced activity and selectivity observed with our supported Au–Pd alloyed catalyst. In

(15) Lee, A. F.; Baddeley, C. J.; Hardacre, C.; Ormerod, M. R.; Lambert, R. M.; Schmid, G.; West, H. J. *Phys. Chem.* **1995**, *99*, 6096.

(16) Takatani, H.; Kago, H.; Kobayashi, Y.; Hori, F.; Oshima, R. *Trans. Mater. Res. Soc. Jpn.* **2003**, *28*, 871.

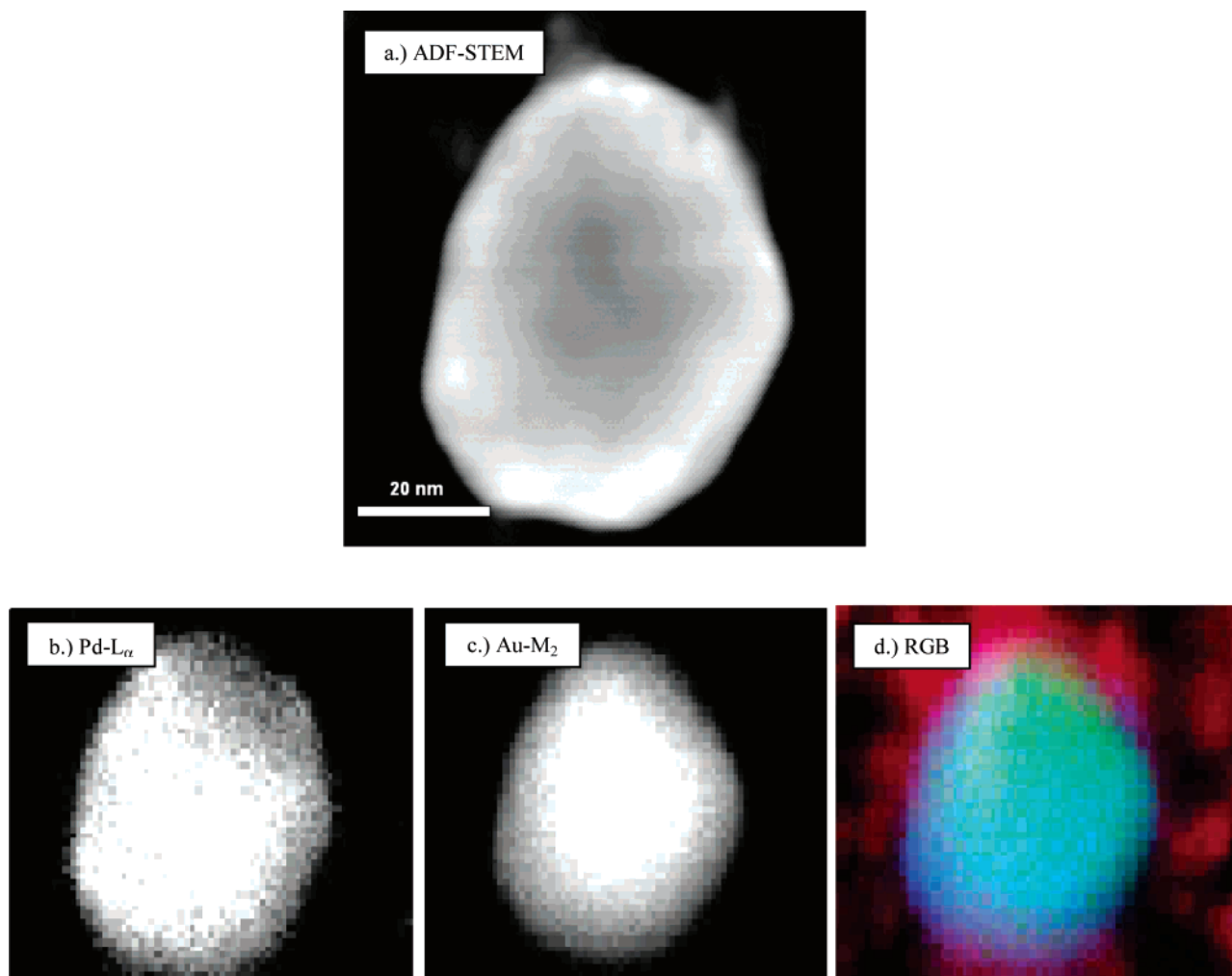


**Figure 4.** Montage of STEM data from a 25 nm particle in the calcined 2.5 wt % Au–2.5 wt % Pd/Al<sub>2</sub>O<sub>3</sub> sample. (a) ADF image with corresponding XEDS maps of (b) Pd L<sub>α</sub>, (c) Au M<sub>2</sub>, and (d) reconstructed RGB (red = Al, green = Au, and Pd = blue) image showing preferential surface enrichment of Pd.

addition, the increase in the size distribution of the Au–Pd nanoparticles appears to be associated with a dramatic increase in the catalytic performance for hydrogen peroxide synthesis. Interestingly, we note that the most effective catalysts for the synthesis of hydrogen peroxide are inactive for CO oxidation, indicating that the active sites for these two reactions may be different. CO oxidation is considered to proceed best with catalysts that comprise relatively small Au nanoparticles (ca 2–5 nm), but there may also be involvement of cationic gold in the reaction mechanism.<sup>17</sup> An alternative explanation for the inverse relationship between catalysts that promote CO oxidation and those that can synthesize H<sub>2</sub>O<sub>2</sub> is the existence of residual chlorine in the catalysts made by impregnation. The Cl K<sub>α</sub> STEM-XEDS map shown in Figure 3d shows that there is clearly a strong spatial correlation between chlorine and many of the Au–Pd alloy particles. This is not surprising since the precursors for both Pd and Au used during impregnation were chloride-based (i.e., HAuCl<sub>4</sub>·3H<sub>2</sub>O and PdCl<sub>2</sub>). It is generally agreed that residual chloride can adversely affect CO oxidation activity.

Our results from this study suggest that larger (i.e., ≥10 nm diameter) Au–Pd particles with a core–shell structure may be the most effective catalysts for H<sub>2</sub>O<sub>2</sub> production, thereby accounting for the differences in activity associated with the aged and fresh catalysts observed with this support.

### Conclusion

In a detailed study of alumina supported Au–Pd catalysts for the direct oxidation of H<sub>2</sub> with O<sub>2</sub> to produce H<sub>2</sub>O<sub>2</sub>, it is apparent that stable and reusable catalysts require calcination at 400 °C. Catalysts pretreated at lower temperatures are unstable and leach Au and Pd into solution, although they still retain considerable activity. Reduction in H<sub>2</sub> prior to use increases the activity further for the optimum Au–Pd composition. STEM-XEDS analysis indicates that the alloy particles in the selective catalysts have a core–shell structure with a Pd-rich shell, and this is consistent with an XPS analysis of the surface chemistry. Storage of the catalyst leads to an increase in the average particle size, and this is associated with a significant enhancement in catalyst activity.

(17) Kobayashi, Y.; Kiao, S.; Seto, M.; Takatani, H.; Nakanishi, M.; Oshima, T. *Hyperfine Interact.* **2004**, 156/157, 75.

**Acknowledgment.** This work formed part of the EU AURICAT project (Contract HPRN-CT-2002-00174) and the

ATHENA project sponsored by the EPSRC and Johnson Matthey PLC, and we thank them for funding this research. We also thank the World Gold Council, for providing funding under the GROW scheme, and Cardiff University for the award of an AA Reed studentship to J.K.E. A.H. and C.J.K. acknowl-

edge the generous support of the NSF Materials Research Science and Engineering Center (NSF DMR 0079996).

CM052633O